

BrainECHO: Semantic Brain Signal Decoding through Vector-Quantized Spectrogram Reconstruction for Whisper-Enhanced Text Generation

Jilong Li¹, Zhenxi Song¹, Jiaqi Wang¹, Min Zhang¹, Zhiguo Zhang¹

¹School of Computer Science and Technology, Harbin Institute of Technology, Shenzhen
200110217@stu.hit.edu.cn, {songzhenxi, zhiguo Zhang}@hit.edu.cn

Abstract

Recent advances in decoding language from brain signals (EEG and MEG) have been significantly driven by pre-trained language models, leading to remarkable progress on publicly available non-invasive EEG/MEG datasets. However, previous works predominantly utilize teacher forcing during text generation, leading to significant performance drops without its use. A fundamental issue is the inability to establish a unified feature space correlating textual data with the corresponding evoked brain signals. Although some recent studies attempt to mitigate this gap using an audio-text pre-trained model, Whisper, which is favored for its signal input modality, they still largely overlook the inherent differences between audio signals and brain signals in directly applying Whisper to decode brain signals. To address these limitations, we propose a new multi-stage strategy for semantic **brain** signal decoding via **v**ector-quantized **s**peCtrogram reconstruction for **W**hisper-enhanced text generati**O**n, termed BrainECHO. Specifically, BrainECHO successively conducts: 1) Discrete *autoencoding* of the audio spectrogram; 2) Brain-audio latent space *alignment*; and 3) Semantic text generation via Whisper *finetuning*. Through this *autoencoding–alignment–finetuning* process, BrainECHO outperforms state-of-the-art methods under the same data split settings on two widely accepted resources: the EEG dataset (*Brennan*) and the MEG dataset (*GWilliams*). The innovation of BrainECHO, coupled with its robustness and superiority at the sentence, session, and subject-independent levels across public datasets, underscores its significance for language-based brain-computer interfaces.

Introduction

Decoding text from brain activity, such as electroencephalography (EEG) and magnetoencephalography (MEG), is a critical and frontier research topic, that can provide a foundation for language-based brain-computer interfaces (BCI) by enabling direct text input through brain signals. In the long term, accurate real-time translation of human brain signals can promote the widespread application of BCI technology in medicine, assistive technology, and entertainment, bringing new possibilities to human life.

With the rapid developments in natural language processing (NLP), automatic speech recognition (ASR), and other fields, researchers have leveraged the powerful language understanding and generating capabilities of pretrained large

language models (LLMs) for neural decoding tasks (Wang and Ji 2022; Duan et al. 2024; Yang et al. 2024a,b), making it possible to accurately decode text stimuli from non-invasive signals. EEG-to-Text (Wang and Ji 2022) is the first work to decode open-vocabulary tokens from encoded word-level EEG rhythm features with the pretrained large model BART (Lewis et al. 2020). Furthermore, DeWave (Duan et al. 2024) used sentence-level raw EEG signals to perform EEG-to-text decoding without eye movement event markers.

Later on, several BART-based methods (Xi et al. 2023; Feng et al. 2023; Amrani, Micucci, and Napoletano 2024) were introduced, predominantly employing a pretraining-finetuning paradigm. These methods first align EEG representations with pretrained text embeddings before feeding them into BART for finetuning. Although these approaches have yielded impressive results, they rely on a teacher-forcing generation strategy, wherein the model depends on the ground truth preceding text during each token prediction. This setting does not accurately reflect the model’s performance in real-world scenarios. These methods show poor decoding performance without teacher forcing.

To address this limitation, NeuSpeech (Yang et al. 2024a) and MAD (Yang et al. 2024b) treat raw MEG signals as a specialized form of speech, transforming MEG signals and feeding them into a pre-trained Whisper model (Radford et al. 2023), which is trained on large-scale audio-text pairs, for end-to-end text decoding without teacher forcing. However, these approaches primarily focus on mapping continuous brain signals to discrete text without compressing the signals into discrete representations, thereby limiting the model’s decoding accuracy and generalization capabilities.

Extensive researches in speech recognition (Zhang et al. 2023a; Puvvada et al. 2024) demonstrate that discrete representations preserve more semantic information for translation compared to conventional speech features like Fbank, thanks to their carefully designed self-supervised learning paradigms. While DeWave (Duan et al. 2024) aligns discrete representations of input EEG signals and text, it assumes a chronological order for the discrete token sequence, requiring a highly capable feature extractor. Considering the natural temporal alignment between audio-evoked brain signals and audio stimuli, aligning raw signals and speech within a discrete space leverages implicit temporal properties, thereby reducing the difficulty of training.

Therefore, we propose a novel multi-stage semantic decoding framework for EEG/MEG **brain** signals, aurally evoked by semantic audio, through vEctor-quantized speCtrogram reconstruction for WHisper-enhanced text generatiOn, termed **BrainECHO**. Specifically, BrainECHO executes the following steps: 1) Discrete *autoencoding* of the audio spectrogram, particularly employing codebook-based vector quantization, to establish a pre-warmed representation space that facilitates Mel spectrogram reconstruction; 2) Brain-audio latent space *alignment*, utilizing a brain encoder and pre-warmed quantizer and decoder to reconstruct the evoked brain signal’s Mel spectrogram; 3) Semantic text generation, achieved through AdaLoRA-based *finetuning* of the pre-trained Whisper model, with the reconstructed Mel spectrogram as input. The overall three-stage (*autoencoding, alignment, finetuning*) training process of the proposed BrainECHO is illustrated in Figure 1. We validate the performance of BrainECHO using two different public audio-evoked brain signal datasets: *Brennan*, which contains EEG data, and *GWilliams*, which contains MEG data. The principal contributions of our work are summarized below:

- The proposed BrainECHO framework overcomes the current flaw in EEG/MEG-to-text approaches that mistakenly rely on the teacher-forcing strategy. It achieves semantic decoding with significantly improved results compared to using Gaussian noise as the input.
- We propose breaking down the EEG/MEG-to-text task into a multi-stage strategy to mitigate the biases induced by the overwhelming capabilities of large language models, while still leveraging their pre-trained knowledge, specifically utilizing Whisper in our work.
- We introduce vector-quantized discrete representations to enhance the model’s efficiency, achieving state-of-the-art (SOTA) performance on EEG and MEG datasets. Specifically, we evaluate BrainECHO across various data split scenarios, which are neglected in prior research.

Related Works

Non-invasive brain signals such as EEG and MEG offer significant advantages over invasive alternatives, particularly in terms of safety and cost-effectiveness. Significant progress has been made in decoding text from non-invasive signals.

Closed-Vocabulary Neural Decoding Ghazaryan et al. (Ghazaryan et al. 2023) utilized Word2vec to decode 60 nouns from MEG recordings. Meta (Défossez et al. 2023) developed a model employing wav2vec 2.0 (Baevski et al. 2020) and contrastive learning to decode speech from 3-second EEG/MEG signals. However, these methods are constrained to closed-vocabulary tasks, restricting their applicability in open-vocabulary text generation.

Decoder-Only Architectures for Open-Vocabulary Brain-to-Text Decoding Recent advancements have leveraged the powerful understanding and generation capabilities of pretrained models, particularly LLMs, to extend vocabulary from closed to open. In decoder-only architectures, some researchers have aligned brain signals

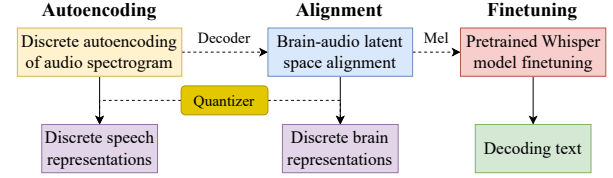


Figure 1: Learning process overview of our proposed BrainECHO framework. BrainECHO follows a three-stage *autoencoding–alignment–finetuning* paradigm: **Autoencoding** stage is used to warm up the Mel spectrogram reconstruction by employing a codebook-based quantizer to enhance generalizability and robustness. This stage especially focuses on exploiting discrete representations. **Alignment** stage reconstructs the Mel spectrogram from the corresponding aurally evoked brain signals. This involves designing a new brain encoder that integrates with the warmed-up quantizer and decoder from the first stage. **Finetuning** stage leverages the capabilities of the pre-trained Whisper model to achieve audio-text translation.

with text to guide pretrained generative models like GPT in text generation. For example, Zhao et al. (Zhao et al. 2024) mapped fMRI data to text embeddings to iteratively guide GPT-2 in generating text. Similarly, Chen et al. (Chen et al. 2024) used text-aligned fMRI representations as prompts for GPT-2 to decode language information.

Seq2seq Architectures for Open-Vocabulary Brain-to-Text Decoding Wang et al. (Wang and Ji 2022) fed transformed word-level EEG rhythm features into a pretrained BART model to decode open-vocabulary tokens. Duan et al. (Duan et al. 2024) integrated discrete EEG encodings with text-EEG contrastive alignment to mitigate individual variability in brain activity. However, these BART-based methods rely on teacher forcing during inference. Furthermore, as Jo et al. (Jo et al. 2024) demonstrated, their performance on noisy data is comparable to that on EEG data, suggesting that these models may simply memorize the training data. Recently, NeuSpeech (Yang et al. 2024a) directly fed raw MEG signals into a modified, pretrained Whisper model for text decoding without teacher forcing. Furthermore, MAD (Yang et al. 2024b) introduced MEG-speech alignment loss to decode sentences not present in the training data. However, these Whisper-based methods do not utilize discrete representations of the original signals to enhance the model’s generalization capabilities. Our work integrates brain-audio discretization and alignment, aiming to predict high-quality Mel spectrograms from brain signals that align with Whisper’s input format. Leveraging Whisper’s advanced speech recognition abilities, our approach generates sentences that closely mirror the original text.

Method

Task Definition

Given the raw EEG/MEG E , text content T , and corresponding audio stimuli A , the experimental data can be divided into a series of sentence-level EEG/MEG-text-speech pairs

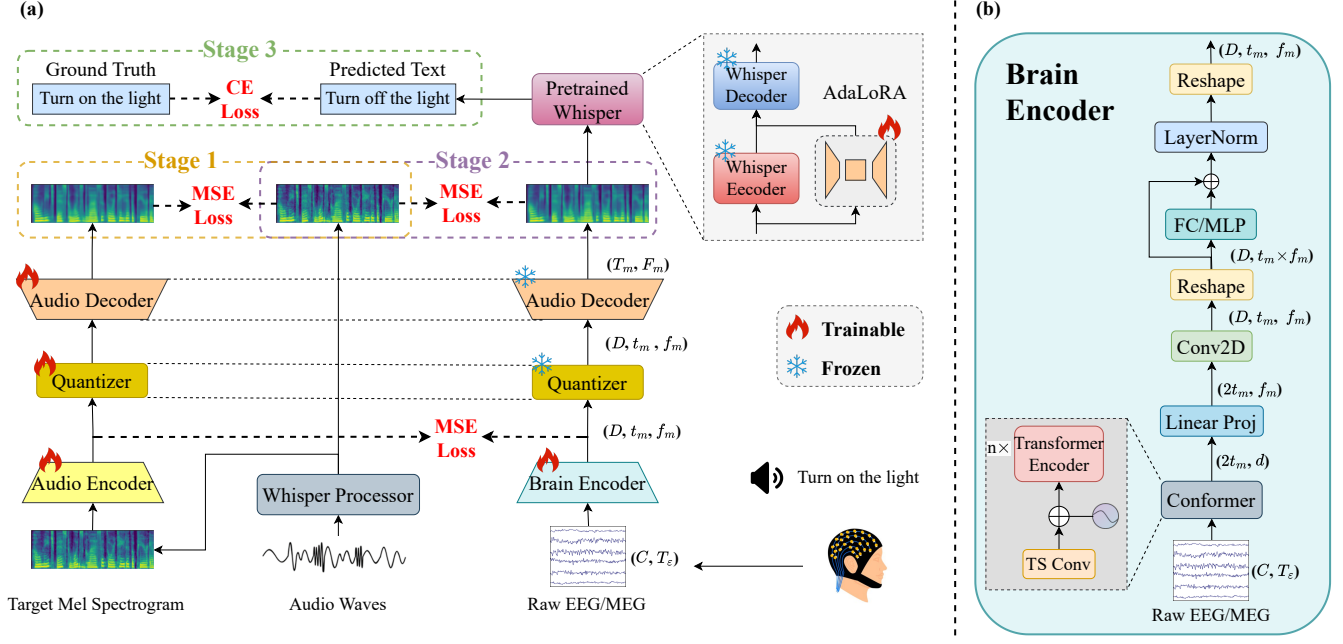


Figure 2: (a) Overview of the BrainECHO model framework. BrainECHO utilizes a three-stage training paradigm consisting of Mel spectrogram autoencoding, brain-audio latent space alignment and Whisper finetuning. C, T_e denotes numbers of raw wave channels and timestamps, respectively. (b) Details of the Brain Encoder, which converts raw EEG/MEG signals into latent representations. d represents the dimension of hidden states and TS Conv stands for Spatio-Temporal Convolution Networks. More details of Conformer are provided in the Appendix.

$\langle \varepsilon, t, a \rangle$ according to T . Our goal is to decode the corresponding open-vocabulary tokens t from the brain signal ε , with a serving as auxiliary information.

Model Architecture

Unlike the multi-task joint training employed in MAD (Yang et al. 2024b), BrainECHO adopts a three-stage training process. This method reduces resource consumption at each training step and facilitates the prediction of high-quality, high-resolution Mel spectrograms from brain signals. Specifically, we extend the spectrogram duration from 3 seconds, as used in (Défossez et al. 2023; Yang et al. 2024b), to over 10 seconds, enabling sentence-level rather than segment-level brain-to-text translation, thereby preserving the semantics of the original sentences. The details of the model are shown in Figure 2. The following sections will detail each training stage.

Discrete Autoencoding of Audio Spectrogram Van den Oord et al. introduced the Vector Quantized-Variational AutoEncoder (VQ-VAE) (Van Den Oord, Vinyals et al. 2017) to learn discrete latent representations of audio, video, and other data types. Building on this approach, several studies (Li, Jia, and Chiu 2023; Sadok, Leglaive, and Séguier 2023; Yang et al. 2023) have explored representing Mel spectrograms using discrete tokens to capture phoneme-like information. Inspired by these methods, our first stage involves autoencoding Mel spectrograms, with the purpose of obtaining a discrete representation space that is con-

ducive to Mel reconstruction. Specifically, given a spectrogram $m \in \mathbb{R}^{T_m \times F_m}$, the audio encoder Enc first converts it into a feature map $z_m = Enc(m) \in \mathbb{R}^{t_m \times f_m \times D}$, where T_m, F_m and D denote the number of time frames, frequency bins and latent channels, respectively. The spectrogram is generated by the Whisper Processor, enabling text decoding from the reconstructed spectrogram using Whisper’s encoder-decoder architecture. Then, z_m is processed by a vector quantizer Q . Specifically, each latent embedding $z_m^{ij} \in \mathbb{R}^D$ ($1 \leq i \leq t_m, 1 \leq j \leq f_m$) is replaced by the nearest vector z_q^{ij} from a codebook $\mathcal{C} \in \mathbb{R}^{N \times D}$, which consists of N learnable D -dimensional vectors. Formally, this process is expressed as follows:

$$Q(z_m^{ij}) = z_q^{ij} = c_k, \text{ where } k = \arg \min_{k \in \{1, 2, \dots, N\}} \|z_m^{ij} - c_k\|_2. \quad (1)$$

The reconstructed spectrogram is then obtained by the audio decoder Dec as: $\hat{m} = Dec(z_q)$. The encoder and decoder are both composed of ResUNet blocks (Kong et al. 2021). The training objective at this stage is defined as follows:

$$L_1 = \|m - \hat{m}\|_2^2 + \alpha \|sg(z_m) - z_q\|_2^2 + \beta_1 \|z_m - sg(z_q)\|_2^2, \quad (2)$$

where $sg(\cdot)$ is a function for stopping gradients, and α, β_1 are hyperparameters for the quantization loss and commitment loss weights, respectively.

Brain-Audio Latent Space Alignment In the second stage, we freeze all the modules pre-trained in the previous

stage and train a brain encoder to convert raw EEG/MEG signals ε into latent features z_ε . The brain encoder utilizes a Conformer-based architecture (Song et al. 2022), which begins with Spatio-Temporal Convolutional Networks to process the input signals into a one-dimensional embedding sequence. The spatial convolutional layer reduces the number of input signal channels to one, while the temporal convolutional layers downsample the time dimension. This sequence is then added to learnable position embeddings and fed into a stack of Transformer encoder blocks. Linear layers and 2D convolutional networks subsequently transform the EEG/MEG features into representations matching the shape of z_m . Similarly, z_ε is input into the frozen quantizer Q and audio decoder Dec to predict the corresponding Mel spectrogram m . Additionally, we align the representations of the Mel spectrogram and raw signals in the latent space. Notably, we employ a unified codebook to leverage pre-warmed discrete acoustic tokens for representing brain activity. The introduction of vector quantization enhances the stability and generalization of the Mel spectrogram reconstruction from brain signals, thereby improving the performance of subsequent text decoding. Formally, the loss for stage 2 is designed as follows:

$$L_2 = \|m - Dec(Q(z_\varepsilon))\|_2^2 + \gamma \|z_m - z_\varepsilon\|_2^2 + \beta_2 \|z_\varepsilon - sg(Q(z_\varepsilon))\|_2^2, \quad (3)$$

where γ and β_2 are used to scale the latent alignment loss and the commitment loss, respectively. The intermediate representations of the codebook and speech provide additional supervisory signals to guide the generation of Mel spectrograms. We employ L2 loss rather than CLIP loss (Défossez et al. 2023; Yang et al. 2024b) to generate highly restored spectrograms that match Whisper’s input.

Whisper Finetuning After obtaining the predicted Mel spectrogram, it is fed into the pretrained Whisper-base model to decode tokens. To adequately leverage the pre-trained knowledge embedded in Whisper, we utilize AdaLoRA (Zhang et al. 2023b), as employed in NeuSpeech (Yang et al. 2024a) and MAD (Yang et al. 2024b), to fine-tune its encoder while keeping the remaining parameters frozen. The objective in this final stage is to minimize the cross-entropy loss between the predicted sentence and the ground truth t .

Experiments

Dataset

The *Brennan* dataset (Brennan and Hale 2019) comprises 49 human EEG recordings, of which 33 remained after screening. Participants passively listened to a 12.4-minute audiobook recording while their EEG signals were recorded. The *GWilliams* (Gwilliams et al. 2023) dataset contains raw MEG recordings from 27 English speakers who listened to naturalistic stories for 2 hours. More details of the datasets are provided in the Appendix.

Preprocess

Brain signals in both datasets are preprocessed similarly. The EEG signals are notch-filtered at 60 Hz and bandpass-

filtered between 0.5 and 99 Hz, and then resampled to 200 Hz. The MEG signals are notched at 50 Hz, filtered with 1~58 Hz and resampled to 100 Hz. Both datasets are normalized to a range of -1 to 1 using robust scalar.

All audio is resampled to 16,000 Hz to align with Whisper’s pretraining configuration. To assess the robustness of our proposed method, we employ different approaches to generate samples. For the *Brennan* dataset, we utilize WhisperX (Bain et al. 2023), a time-accurate speech recognition system, to segment the audio into chunks of up to 12 seconds. For the *GWilliams* dataset, we split the audio according to the original annotations, resulting in segments no longer than 24 seconds. This process generates a series of EEG/MEG-text-speech pairs.

The Whisper processor then converts the speech into an 80-channel Mel spectrogram m using 25-ms windows with a stride of 10 ms. To standardize settings and reduce memory usage, the length of the Mel spectrograms in *GWilliams* is downsampled to half its original value, resulting in m having a consistent shape of (80, 1200). Finally, we obtain 140 and 661 unique sentences from the two datasets, respectively.

Dataset Splitting and Validation Strategies

Individual differences and attention levels of subjects can affect EEG signals, making it difficult for models to generalize across subjects and trials. To explore the model’s generalization ability, we design different dataset splitting and validation strategies: random shuffling, session-based, sentence-based, and subject-based splittings. More details are provided in the Appendix. Unless otherwise specified, the *Brennan* and *GWilliams* datasets are partitioned by subject-based splittings and random shuffling, respectively, in the following presented results.

Implementation Details

The models are trained on Nvidia 3090 GPUs (24GB). Training on the *Brennan* and *GWilliams* datasets take approximately 4 and 24 hours, respectively, using a single GPU. The hyperparameters are set as follows: $\alpha = 0.5$, $\beta_1 = \beta_2 = 0.1$, $\gamma = 1$, $N = 2048$, $d = 256$, and $D = 8$. The audio encoder is configured with a downsampling rate of 4. We use vanilla Transformer encoder with 4 layers and 8 heads. All EEG/MEG samples are zero-padded to 2400 in the time dimension. Input spectrograms are padded uniformly to a length of 3000 with -1 following Whisper’s configuration. For the *GWilliams* dataset, the length of the predicted Mel spectrogram is upsampled by a factor of 2. When generating with Whisper, we set the number of beams to 5 for beam search and apply a repetition penalty of 5.0 with a no-repeat n-gram size of 2. Further details on the training configuration are provided in the Appendix.

Experimental Results

Overall Comparison We use BLEU (Papineni et al. 2002), ROUGE-1 (Lin 2004) and Word Error Rate (WER) to evaluate decoding performance. BLEU and ROUGE-1 are used to evaluate the quality of text generation, while WER is used to calculate error rate based on edit distance. As shown

Input	Method	BLEU-N (%) \uparrow				ROUGE-1 (%) \uparrow			WER (%) \downarrow
		N=1	N=2	N=3	N=4	P	R	F	
Noise	NeuSpeech (Yang et al. 2024a)	8.45	1.78	0.43	0	10.26	21.61	13.02	198.31
Noise	BrainECHO	4.75	1.10	0.28	0	11.25	7.81	8.52	105.27
EEG feature	EEG-to-Text (Wang and Ji 2022)	8.82	3.15	1.90	1.44	10.13	21.61	13.12	233.99
EEG	NeuSpeech (Yang et al. 2024a)	85.31	84.38	83.98	83.75	82.60	82.73	82.64	16.97
EEG	BrainECHO	89.78	89.06	88.74	88.55	87.05	87.27	87.13	11.72
EEG	NeuSpeech (Yang et al. 2024a) w/ <i>tf</i>	93.77	93.51	93.25	92.98	95.41	98.09	96.43	6.55
EEG	BrainECHO w/ <i>tf</i>	98.82	98.74	98.68	98.64	98.45	98.44	98.45	1.18

Table 1: Overall comparison of decoding performance on the *Brennan* dataset. By default, all methods are evaluated without teacher forcing. The metrics with teacher forcing (w/ *tf*) are further explored. Further results are in the Appendix.

Dataset	Split	BLEU-N (%) \uparrow			
		N=1	N=2	N=3	N=4
<i>Brennan</i>	Subject	89.78	89.06	88.74	88.55
	Sentence	89.24	88.52	88.18	88.01
<i>GWilliams</i>	RS	73.35	72.66	72.46	72.42
	Session	75.24	74.57	74.34	74.27
	Subject	75.05	74.38	74.18	74.14
	Sentence	73.58	72.99	72.82	72.79

Table 2: Comparison of decoding performance on different datasets and splits. RS denotes random shuffling.

in Table 1, we compare our model with popularly-referred brain-to-text architectures, EEG-to-Text (Wang and Ji 2022) and NeuSpeech (Yang et al. 2024a). Obviously, our method demonstrates remarkable decoding performance, achieving BLEU- $\{1, 2, 3, 4\}$ of 89.78, 89.06, 88.74 and 88.55, as well as WER of 11.27 without teacher forcing. The results indicate that BrainECHO generates text highly consistent with the ground truth. Specifically, in terms of BLEU-4, BrainECHO outperforms the previous baseline and current SOTA method by 87.11 (+6049%) and 4.8 (+5.73%) respectively. When using teacher forcing, BrainECHO achieves BLEU-4 of 98.45, which is nearly perfect, highlighting the unrealistic metrics produced by teacher forcing evaluation.

Additionally, when random Gaussian noise is input into BrainECHO, the translation metrics are significantly low, indicating that BrainECHO captures the intrinsic connection between brain signals and text, rather than simply memorizing sentences from the training set. Intuitively, BrainECHO is more resistant to noise than NeuSpeech (Yang et al. 2024a). Notably, the model ideally should not respond to noise, with a WER expected to be 1. Therefore, a high WER (> 1), suggesting the model outputs excessive irrelevant content, is not necessarily a desirable result.

Different Datasets and Splitting Strategies The decoding metrics of BrainECHO across different datasets and splitting strategies are shown in Table 2. The model demonstrates optimal performance on the *Brennan* and *GWilliams* dataset when split by sentences and sessions, respectively. Notably, the performance differences across various splitting

Split	Autoencode	BLEU-N (%) \uparrow			
		N=1	N=2	N=3	N=4
Subject	Separate	89.78	89.06	88.74	88.55
	Joint	89.79	89.08	88.73	88.55
Sentence	Separate	89.24	88.52	88.18	88.01
	Joint	89.91	89.22	88.88	88.69

Table 3: Comparison of decoding performance using separate and joint autoencoding on the *Brennan* dataset. By default, we employ separate autoencoding.

strategies are not significant, indicating that BrainECHO is robust and effectively alleviates covariate shift among different subjects or trials without the need for external information (e.g., subject or trial identifiers), provided that all unique sentences are encountered during training. In contrast, the brain module used in (Défossez et al. 2023; Yang et al. 2024b) employs distinct projection matrices for each subject to mitigate individual differences, yet it cannot be generalized to unseen subjects directly.

Examples of Generated Sentences Some samples generated from different methods are shown in Table 4. These examples indicate that BrainECHO can produce sentences that closely match the original text, even when the reference is long and complex. Remarkably, even without the final fine-tuning of Whisper, BrainECHO still generates results highly relevant to the original text, highlighting the effectiveness of brain-audio latent space alignment (stage 2). In contrast, EEG-to-Text (Wang and Ji 2022) struggles to generate semantically relevant sentences, and NeuSpeech (Yang et al. 2024a) may generate content unrelated to the ground truth when decoding long sentences, which significantly impacts practical applications.

Ablation Study and Analysis

Autoencoding We compare the decoding performance when the autoencoding task (stage 1) is applied separately to the Mel spectrograms from individual datasets versus both datasets combined. The results, presented in Table 3, indicate that joint autoencoding results in either stable or slightly improved metrics (except for BLEU-3) compared to sepa-

Generated samples on <i>Brennan</i> (Brennan and Hale 2019)		
(1)	Ground Truth	There seemed to be no use in waiting by the little door, so she went back to the table.
	EEG-to-Text (Wang and Ji 2022)	But they were all locked, and when Alice had been all the way down one side and up the other trying every door, she did not care how she was ever to get out again.
	NeuSpeech (Yang et al. 2024a)	There seemed to be no use in waiting by the little door, so she went back to the table.
	BrainECHO <i>w/o ft</i>	There seemed to be no use in waiting by the little door, so she went back to the table.
	BrainECHO	There seemed to be no use in waiting by the little door, so she went back to the table.
(2)	Ground Truth	that she'd never before seen a rabbit with either a waistcoat pocket or a watch to take out of it, and burning with curiosity, she ran across the field after it, and fortunately
	EEG-to-Text (Wang and Ji 2022)	how she longed to get out of that dark hall and wander about among those beds of bright flowers and those cool fountains, but she did not even get her head through the doorway.
	NeuSpeech (Yang et al. 2024a)	But they were all locked, and when Alice had been all the way down one side and up the other trying every door, she walked sadly down the middle, wondering how she was ever to get out again.
	BrainECHO <i>w/o ft</i>	But she will never be foreseen around it, with either a waistcoat pocket or a watch to take out of it and burn in curiosity. She ran across the field after it unfortunately.
	BrainECHO	that she'd never before seen a rabbit with either a waistcoat pocket or a watch to take out of it and burning with curiosity, she ran across the field after it, and fortunately
Generated samples on <i>GWilliams</i> (Gwilliams et al. 2023)		
(1)	Ground Truth	I seen him since high school maybe twenty years before and we were never buddies in the first place
	EEG-to-Text (Wang and Ji 2022)	It was a long time since I had last seen him in the flesh
	NeuSpeech (Yang et al. 2024a)	I seen him since high school when I was young, at least before and we were never buddies in any place.
	BrainECHO <i>w/o ft</i>	I hadn't seen him since high school, maybe 20 years before and you remember when he's in the first place.
	BrainECHO	I seen him since high school maybe twenty years before and we were never buddies in the first place
(2)	Ground Truth	My patience was long gone and I was back in the car to warming up when Acres tapped on the window and told me he had found whatever he was looking for
	EEG-to-Text (Wang and Ji 2022)	<u>He said</u> he had no idea how long it would take him to get back home
	NeuSpeech (Yang et al. 2024a)	My patience was long gone and I was back in the car. But when I heard that many of you were looking for whatever it was, but what about this?
	BrainECHO <i>w/o ft</i>	My patience was long gone, and I was back in the car to warming up when acres tapped on the window and Tunch told me he had found whatever he was looking for.
	BrainECHO	My patience was long gone and I was back in the car to warming up when Acres tapped on the window and told me he had found whatever he was looking for

Table 4: Comparison of decoding sentences generated by different methods, where **bold** and underline respectively indicates an exact match and a similar match between prediction and ground truth. All methods use the same generation configuration. *w/o ft* means decoding by inputting the predicted Mel spectrogram into Whisper directly without fine-tuning in the last stage. Additional examples are provided in the Appendix.

rate autoencoding when splitting *Brennan* by subject. Additionally, all metrics improve when splitting by sentence. This suggests that incorporating Mel spectrograms from other datasets during autoencoding enhances the model's ability to extract richer discrete speech representations, thereby enhancing its generalizability.

Prediction of Mel Spectrogram Examples of Mel spectrograms predicted by BrainECHO are presented in the Appendix. Since reconstructing a 12-second Mel spectrogram from brain signals in a single pass can significantly impact training efficiency and memory usage, we opt to divide the raw signals into n -second segments to balance decoding accuracy and resource consumption. The corresponding Mel spectrogram for each segment is predicted and then concatenated to form a complete one. We experiment with window

Window Length n (s)	BLEU-N (%) \uparrow			
	N=1	N=2	N=3	N=4
12	89.78	89.06	88.74	88.55
6	50.45	45.13	42.54	40.72
4	15.94	5.94	2.60	1.24

Table 5: Decoding comparison for various window lengths in 12-sec Mel spectrogram on *Brennan* dataset.

lengths of $n = \{4, 6, 12\}$, with results shown in Table 5. As the segmentation granularity increases, translation performance gradually deteriorates, indicating that predicting the entire Mel spectrogram at once is more effective than

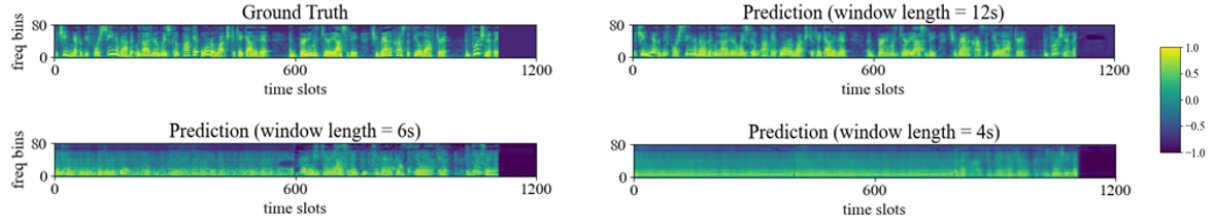


Figure 3: Predicted Mel spectrograms with different window segments on the *Brennan* dataset. The sentence in this figure is:” that she’d never before seen a rabbit with either a waistcoat pocket or a watch to take out of it, and burning with curiosity, she ran across the field after it, and fortunately.”

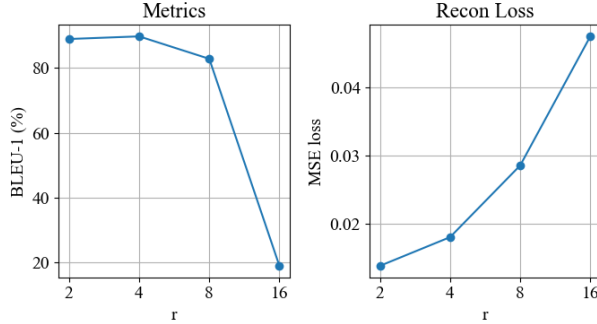


Figure 4: Changes of BLEU-1 and Mel spectrogram reconstruction loss in stage 2 with different downsampling ratio.

segmenting. The latter method disrupts sentence semantics and introduces discontinuities at segment boundaries. Predicted spectrograms are compared in Figure 3, where clear segmentation artifacts are evident with the splitting method. Notably, if the predicted Mel spectrogram lacks silence at the end, the resulting image appears blurry and smooth, an issue that becomes more pronounced as the window length decreases. This suggests that the model constructs a more robust discrete representation space when using complete Mel spectrograms with silent portions.

Downsampling Ratio To assess the impact of the downsampling ratio r , we evaluate BrainECHO’s performance at r values of 2, 4, 8, and 16, while holding other hyperparameters constant. Assuming each pixel in the spectrogram is represented by 8 bits, the corresponding reductions in bit usage are approximately 2.9, 11.6, 46.5, and 186.1, respectively. As illustrated in Figure 4, increasing r exacerbates information loss, making accurate reconstruction of Mel spectrograms for sentence decoding more challenging. Interestingly, the decoding performance at $r = 2$ is not as strong as at $r = 4$, indicating that while a larger feature map enhances reconstruction quality, it may also introduce redundant, translation-irrelevant information, thereby complicating the fine-tuning of Whisper. Therefore, selecting a moderate r is essential to optimize latent representation capacity.

Three Training Stages To verify the effectiveness of our proposed three-stage training, we incrementally remove each stage and observe the corresponding changes in per-

Training Stage			BLEU-N (%) \uparrow			
Au	Al	F	N=1	N=2	N=3	N=4
✓	✓	✓	89.78	89.06	88.74	88.55
✗	✓	✓	87.13	86.29	85.92	85.74
✗	✗	✓	87.63	86.87	86.54	86.38
✓	✓	✗	39.64	34.49	31.07	28.32

Table 6: Ablation study of training stages on the *Brennan* dataset. The stages labeled Au, Al, and F correspond to Mel spectrogram autoencoding, brain-audio latent space alignment, and Whisper fine-tuning, respectively.

formance. As presented in Table 6, when the autoencoding stage is removed—where the quantizer and audio decoder are randomly initialized—BLEU-4 drops to 85.74 (-3.17%). Further removal of the brain-audio alignment stage leads to an abnormal increase in BLEU, highlighting the challenge of directly constructing a representation space from the brain signals to the Mel spectrogram. However, by pre-warming a discrete representation space, the reconstruction quality and stability are enhanced. The most significant decline in performance occurs when the fine-tuning phase is omitted. Notably, even without fine-tuning, BrainECHO achieves impressive performance based solely on the predicted Mel spectrogram, suggesting that excessive fine-tuning of Whisper is unnecessary, as it could result in overfitting.

Conclusion

This paper introduces a novel three-stage brain-to-text framework, BrainECHO, that addresses the shortcomings of prior methods. These methods relied on teacher forcing and failed to compare model performance against pure noise inputs. BrainECHO bridges the latent spaces of text and corresponding aurally evoked brain signals through vector-quantized spectrogram reconstruction and fine-tuned use of the Whisper model. It achieves state-of-the-art (SOTA) performance on public EEG and MEG datasets across various experimental settings. By extracting deep semantic information from brain signals, BrainECHO provides valuable insights for future research in the brain-to-text decoding paradigm in the BCI field.

References

- Amrani, H.; Micucci, D.; and Napoletano, P. 2024. Deep Representation Learning for Open Vocabulary Electroencephalography-to-Text Decoding. *IEEE Journal of Biomedical and Health Informatics*.
- Baevski, A.; Zhou, Y.; Mohamed, A.; and Auli, M. 2020. wav2vec 2.0: A framework for self-supervised learning of speech representations. *Advances in neural information processing systems*, 33: 12449–12460.
- Bain, M.; Huh, J.; Han, T.; and Zisserman, A. 2023. Whisperx: Time-accurate speech transcription of long-form audio. *arXiv preprint arXiv:2303.00747*.
- Brennan, J. R.; and Hale, J. T. 2019. Hierarchical structure guides rapid linguistic predictions during naturalistic listening. *PloS one*, 14(1): e0207741.
- Chen, X.; Du, C.; Liu, C.; Wang, Y.; and He, H. 2024. Open-vocabulary Auditory Neural Decoding Using fMRI-prompted LLM. *arXiv preprint arXiv:2405.07840*.
- Défossez, A.; Caucheteux, C.; Rapin, J.; Kabeli, O.; and King, J.-R. 2023. Decoding speech perception from non-invasive brain recordings. *Nature Machine Intelligence*, 5(10): 1097–1107.
- Duan, Y.; Chau, C.; Wang, Z.; Wang, Y.-K.; and Lin, C.-t. 2024. Dewave: Discrete encoding of eeg waves for eeg to text translation. *Advances in Neural Information Processing Systems*, 36.
- Feng, X.; Feng, X.; Qin, B.; and Liu, T. 2023. Aligning semantic in brain and language: A curriculum contrastive method for electroencephalography-to-text generation. *IEEE Transactions on Neural Systems and Rehabilitation Engineering*.
- Ghazaryan, G.; van Vliet, M.; Saranpää, A.; Lammi, L.; Lindh-Knuutila, T.; Hultén, A.; Kivisaari, S.; and Salmelin, R. 2023. Trials and tribulations when attempting to decode semantic representations from MEG responses to written text. *Language, Cognition and Neuroscience*, 1–12.
- Gwilliams, L.; Flick, G.; Marantz, A.; Pykkänen, L.; Poeppel, D.; and King, J.-R. 2023. Introducing MEG-MASC a high-quality magneto-encephalography dataset for evaluating natural speech processing. *Scientific data*, 10(1): 862.
- Jo, H.; Yang, Y.; Han, J.; Duan, Y.; Xiong, H.; and Lee, W. H. 2024. Are EEG-to-Text Models Working? *arXiv preprint arXiv:2405.06459*.
- Kong, Q.; Cao, Y.; Liu, H.; Choi, K.; and Wang, Y. 2021. Decoupling magnitude and phase estimation with deep resnet for music source separation. In *22nd International Conference on Music Information Retrieval, ISMIR 2021*, 342–349. International Society for Music Information Retrieval.
- Lewis, M.; Liu, Y.; Goyal, N.; Ghazvininejad, M.; Mohamed, A.; Levy, O.; Stoyanov, V.; and Zettlemoyer, L. 2020. BART: Denoising Sequence-to-Sequence Pre-training for Natural Language Generation, Translation, and Comprehension. In *Proceedings of the 58th Annual Meeting of the Association for Computational Linguistics*, 7871–7880.
- Li, X.; Jia, Y.; and Chiu, C.-C. 2023. Textless direct speech-to-speech translation with discrete speech representation. In *ICASSP 2023-2023 IEEE International Conference on Acoustics, Speech and Signal Processing (ICASSP)*, 1–5. IEEE.
- Lin, C.-Y. 2004. Rouge: A package for automatic evaluation of summaries. In *Text summarization branches out*, 74–81.
- Papineni, K.; Roukos, S.; Ward, T.; and Zhu, W.-J. 2002. Bleu: a method for automatic evaluation of machine translation. In *Proceedings of the 40th annual meeting of the Association for Computational Linguistics*, 311–318.
- Puvvada, K. C.; Koluguri, N. R.; Dhawan, K.; Balam, J.; and Ginsburg, B. 2024. Discrete Audio Representation as an Alternative to Mel-Spectrograms for Speaker and Speech Recognition. In *ICASSP 2024-2024 IEEE International Conference on Acoustics, Speech and Signal Processing (ICASSP)*, 12111–12115. IEEE.
- Radford, A.; Kim, J. W.; Xu, T.; Brockman, G.; McLeavey, C.; and Sutskever, I. 2023. Robust speech recognition via large-scale weak supervision. In *International conference on machine learning*, 28492–28518. PMLR.
- Sadok, S.; Leglaive, S.; and Séguier, R. 2023. A vector quantized masked autoencoder for speech emotion recognition. In *2023 IEEE International conference on acoustics, speech, and signal processing workshops (ICASSPW)*, 1–5. IEEE.
- Song, Y.; Zheng, Q.; Liu, B.; and Gao, X. 2022. EEG conformer: Convolutional transformer for EEG decoding and visualization. *IEEE Transactions on Neural Systems and Rehabilitation Engineering*, 31: 710–719.
- Van Den Oord, A.; Vinyals, O.; et al. 2017. Neural discrete representation learning. *Advances in neural information processing systems*, 30.
- Wang, Z.; and Ji, H. 2022. Open vocabulary electroencephalography-to-text decoding and zero-shot sentiment classification. In *Proceedings of the AAAI Conference on Artificial Intelligence*, 5350–5358.
- Xi, N.; Zhao, S.; Wang, H.; Liu, C.; Qin, B.; and Liu, T. 2023. UniCoRN: Unified Cognitive Signal Reconstruction bridging cognitive signals and human language. *arXiv preprint arXiv:2307.05355*.
- Yang, D.; Yu, J.; Wang, H.; Wang, W.; Weng, C.; Zou, Y.; and Yu, D. 2023. DiffSound: Discrete diffusion model for text-to-sound generation. *IEEE/ACM Transactions on Audio, Speech, and Language Processing*, 31: 1720–1733.
- Yang, Y.; Duan, Y.; Zhang, Q.; Xu, R.; and Xiong, H. 2024a. Decode neural signal as speech. *arXiv preprint arXiv:2403.01748*.
- Yang, Y.; Jo, H.; Duan, Y.; Zhang, Q.; Zhou, J.; Lee, W. H.; Xu, R.; and Xiong, H. 2024b. MAD: Multi-Alignment MEG-to-Text Decoding. *arXiv preprint arXiv:2406.01512*.
- Zhang, D.; Ye, R.; Ko, T.; Wang, M.; and Zhou, Y. 2023a. DUB: Discrete Unit Back-translation for Speech Translation. In *Findings of the Association for Computational Linguistics: ACL 2023*, 7147–7164.
- Zhang, Q.; Chen, M.; Bukharin, A.; Karampatziakis, N.; He, P.; Cheng, Y.; Chen, W.; and Zhao, T. 2023b. AdaLoRA: Adaptive budget allocation for parameter-efficient fine-tuning. *arXiv preprint arXiv:2303.10512*.

Zhao, X.; Sun, J.; Wang, S.; Ye, J.; Xhz, X.; and Zong, C. 2024. MapGuide: A Simple yet Effective Method to Reconstruct Continuous Language from Brain Activities. In *Proceedings of the 2024 Conference of the North American Chapter of the Association for Computational Linguistics: Human Language Technologies (Volume 1: Long Papers)*, 3822–3832.

Appendix

A. Conformer

Conformer utilizes a Convolution-Transformer architecture to capture both local and global features. The one-dimensional temporal and spatial convolution layers in TS Conv capture the local information of neural signals, while the self-attention modules in the Transformer blocks extract the global dependencies of these local time features. The detailed structure of Conformer is provided in Table 7.

B. Dataset

B.1 Brennan

The *Brennan* dataset (Brennan and Hale 2019) contains raw electroencephalography (EEG) data collected from 49 human subjects. Participants were asked to passively listen to a 12.4-minute audiobook story of chapter one of *Alice’s Adventures in Wonderland*, while their EEG data was recorded. Participants completed an eight-question multiple choice questionnaire concerning the contents of the story at the end of the experimental session. We retain 33 participants’ data who achieved high scores.

Participants were fitted with an elastic cap with 61 actively-amplified electrodes and one ground electrode (actiCap, Brain Products GmbH). Electrodes were distributed equidistantly across the scalp according to the Easycap M10 layout. Conductive gel was inserted into each electrode to reduce impedances to 25 kOhms or below. Data were recorded at 500 Hz between 0.1 and 200 Hz referenced to an electrode placed on the right mastoid (actiCHamp, Brain Products GmbH).

The stimulus chapter originally contains 84 sentences. Since the annotation files only provide word-level annotations, directly concatenating words to form sentences would result in the absence of punctuation marks. Therefore, we use WhisperX (Bain et al. 2023) to segment the audio stimulus into segments of no more than 12 seconds, resulting in 140 sentences.

B.2 GWilliams

GWilliams (Gwilliams et al. 2023), known as the “MEG-MASC” dataset, provides raw magnetoencephalography (MEG) data from 27 English speakers who listened to two hours of naturalistic stories. Each participant performed two identical sessions, involving listening to four fictional stories from the Manually Annotated Sub-Corpus (MASC). The four stories are: ‘LW1’ (861 words, 5 min 20 sec), ‘Cable Spool Boy’ (1948 words, 11 min), ‘Easy Money’ (3541 words, 12 min 10 sec) and ‘The Black Willow’ (4652 words, 25 min 50 sec).

An audio track corresponding to each of these stories was synthesized using Mac OS Mojave © version 10.14 text-to-speech. To help decorrelate language features from acoustic representations, both voices and speech rate were varied every 5–20 sentences. Specifically, three distinct synthetic voices: ‘Ava’, ‘Samantha’ and ‘Allison’ are used speaking between 145 and 205 words per minute. Additionally, the silence between sentences are varied between 0 and 1,000ms.

Both speech rate and silence duration were sampled from a uniform distribution between the min and max values.

Each story was divided into ~ 3 min sound files. In between these sounds—approximately every 30 s—a random word list generated from the unique content words (nouns, proper nouns, verbs, adverbs and adjectives) selected from the preceding 5min segment presented in random order were played.

Within each ~ 1 h recording session, participants were recorded with a 208 axial-gradiometer MEG scanner built by the Kanazawa Institute of Technology (KIT), and sampled at 1,000 Hz, and online band-pass filtered between 0.01 and 200Hz while they listened to four distinct stories through binaural tube earphones (Aero Technologies), at a mean level of 70dB sound pressure level.

To ensure a fair comparison with NeuSpeech (Yang et al. 2024a), we follow its experimental setup by concatenating words with the same sentence ID into full sentences, based on the annotation files. This process results in 661 sentences.

C. Dataset Splitting

In this section, we detail the dataset splitting strategies employed in our study. As shown in Table 8, four distinct strategies are utilized, each presenting different levels of evaluation difficulty. The random shuffling strategy is the most basic, incorporating data from all subjects and trials into the training samples. The sentence-based strategy is more challenging, simulating scenarios where samples from different participants are not aligned, resulting in missing data for some sentences for each participant. The session-based and subject-based strategies are the most difficult but also the most realistic, as they assess the model’s ability to generalize to new trials and subjects, respectively. This capability is crucial for the practical application of language-based BCIs. The *Brennan* dataset utilizes only two splitting methods due to its inclusion of data from a single trial. Consequently, splitting by sentence yields results similar to those obtained by random shuffling.

D. Implementation Details

The training configurations for our model vary across different datasets and training stages. Detailed settings for each training phase are outlined in Table 9. The final model is selected based on the lowest validation loss. Notably, no data augmentation techniques are employed, and no subject-related information is provided to the model.

E. Evaluation Results

Evaluation metrics of the *GWilliams* dataset across various splitting strategies are presented in Table 10. NeuSpeech (Yang et al. 2024a), the previous SOTA model for MEG-to-text translation, serves as the baseline for comparison. Given the similarity in data preprocessing and dataset splitting strategies, the NeuSpeech results are cited directly from the original paper. When using random shuffling, BrainECHO achieves a BLEU-4 score of 72.42, outperforming NeuSpeech by 24.64 points (+51.57%). Additionally, with session-based splitting, BrainECHO attains a

BLEU-1 score of 75.24, exceeding NeuSpeech by 22.08 points (+41.53%). These results indicate that BrainECHO can generate text that closely matches the ground truth.

F. Generated Samples

To intuitively demonstrate the powerful decoding ability of BrainECHO, additional translated examples for the *Brennan* and *GWilliams* datasets are presented in Table 11 and 12, respectively.

G. Reconstructed Mel Spectrograms

Figure 5 and 6 display some samples of Mel spectrograms reconstructed from the brain signals for the *Brennan* and *GWilliams* datasets, respectively. These samples demonstrate that BrainECHO can produce Mel spectrograms that are largely consistent with the ground truth. Notably, the model effectively restores fine details and accurately predicts the intervals and silent segments in the spectrograms. These results highlight the model’s expressive and predictive capabilities, as it can extract Mel spectrograms from brain signal segments exceeding 20 seconds—a feat not achieved by previous methods.

H. Codebook Size

To explore the impact of the quantizer, we investigate the performance of BrainECHO with codebook sizes ranging from 1024 to 4096. As shown in Figure 7, the performance peaks at a codebook size of 4096. However, the metrics do not increase linearly with codebook size. When the codebook size increases from 1024 to 2048, the decoding performance improves, but it decreases when the size further increases to 3072. This indicates that a smaller codebook may not capture diverse acoustic representations, while a larger codebook may increase training difficulty and computational burden. Thus, we choose 2048 as the codebook size for balancing performance and efficiency.

Layer Type	Out Channels	Filter Size	Stride	Padding	Input	Output
Conv2D	64	(1, 5)	(1, 2)	2	$1 \times C \times T_\varepsilon$	$64 \times C \times \frac{T_\varepsilon}{2}$
BatchNorm2D + ELU	-	-	-	-	$64 \times C \times \frac{T_\varepsilon}{2}$	$64 \times C \times \frac{T_\varepsilon}{2}$
Conv2D	128	(1, 3)	(1, 2)	1	$64 \times C \times \frac{T_\varepsilon}{2}$	$128 \times C \times \frac{T_\varepsilon}{4}$
BatchNorm2D + ELU	-	-	-	-	$128 \times C \times \frac{T_\varepsilon}{4}$	$128 \times C \times \frac{T_\varepsilon}{4}$
Conv2D	256	(C, 1)	1	0	$128 \times C \times \frac{T_\varepsilon}{4}$	$256 \times C \times \frac{T_\varepsilon}{4}$
BatchNorm2D + ELU	-	-	-	-	$256 \times C \times \frac{T_\varepsilon}{4}$	$256 \times 1 \times \frac{T_\varepsilon}{4}$
Rearrange	-	-	-	-	$256 \times 1 \times \frac{T_\varepsilon}{4}$	$\frac{T_\varepsilon}{4} \times 256$

Table 7: The structure of TS Conv. C and T_ε denote the number of EEG/MEG channels and timestamps, respectively.

Dataset	Split	Details	Result
<i>Brennan</i>	Sentence	For each participant, 10% of unique sentences are allocated to the test set. The remaining sentences are shuffled and split into train:valid 8:1. Note that the test set for each subject may contain different sentences.	3696:462:462
	Subject	3 participants (about 10% of the total number of subjects) are selected at random for the test set, 3 for the validation set, and the remaining 27 for the training set.	3780:420:420
<i>GWilliams</i>	RS	All data is random shuffled and divided into train:valid:test 8:1:1.	23339:2917:2918
	Session	Random shuffled data of session 0 is divided into train:valid 8:1 and data of session 1 is held out as test set.	13129:2976:13069
	Sentence	It is the same as <i>Brennan</i> above.	23305:2914:2955
	Subject	2 participants (about 10% of the total number of subjects) are selected at random for the test set, 2 for the validation set, and the remaining 23 for the training set.	24137:2469:2568

Table 8: Details of different dataset split settings. RS denotes random shuffling.

Configuration	<i>Brennan</i>			<i>GWilliams</i>		
	P	A	F	P	A	F
Batch Size	16	16	16	16	8	16
Max Epoch	400	40	40	100	40	40
Optimizer	AdamW, with weight decay = 1e-2, betas = (0.9, 0.999)					
Max Learning Rate	2e-4	1e-4	1e-4	2e-4	1e-4	2e-4
LR Scheduler	Cosine Annealing, with T_max = Max Epoch					
Early Stopping Patience	4					

Table 9: Details of the experimental configuration. P, A, F denote the various training stages: pretraining, alignment and finetuning, respectively.

Split	Input	Method	BLEU-N (%) \uparrow				ROUGE-1 (%) \uparrow			WER (%) \downarrow
			N=1	N=2	N=3	N=4	P	R	F	
Random Shuffling	MEG feature	EEG-to-Text (Wang and Ji 2022)	9.21	2.13	0.57	0.14	9.74	10.73	11.38	118.25
	MEG	NeuSpeech (Yang et al. 2024a)	60.3	55.26	51.24	47.78	60.88	59.76	58.73	56.63
	MEG	BrainECHO	73.35	72.66	72.46	72.42	69.66	70.12	69.73	31.44
Session	MEG	NeuSpeech (Yang et al. 2024a)	53.16	-	-	-	-	-	-	-
	MEG	BrainECHO	75.24	74.57	74.34	74.27	72.94	72.84	72.78	29.59
Sentence	MEG	BrainECHO	73.58	72.99	72.82	72.79	70.38	70.75	70.73	31.11
Subject	MEG	BrainECHO	75.05	74.38	74.18	74.14	71.83	72.02	71.72	29.80

Table 10: Overall comparison of decoding performance on the *GWilliams* dataset. All methods are evaluated without teacher forcing.

(1)	Ground Truth	There were doors all around the hall.
	Predicted	not much larger than a rat hole.
(2)	Ground Truth	For you see, as she couldn't answer either question, it didn't much matter which way she put it.
	Predicted	For you see, as she couldn't answer either question, it didn't much matter which way she put it.
(3)	Ground Truth	When she thought it over afterwards, it occurred to her that she ought to have wondered at this, but at the time it all seemed quite natural.
	Predicted	When she thought it over afterwards, it occurred to her that she ought to have wondered at this, but at the time it all seemed quite natural.
(4)	Ground Truth	I wonder how many miles I've fallen by this time, she said aloud.
	Predicted	I wonder how many miles I've fallen by this time, she said aloud.
(5)	Ground Truth	and that if you cut your finger very deeply with a knife, it usually bleeds.
	Predicted	and that if you cut your finger very deeply with a knife, it usually bleeds.
(6)	Ground Truth	I can creep under the door, so either way I'll get into the garden, and I don't care which happens.
	Predicted	I can creep under the door, so either way I'll get into the garden, and I don't care which happens.
(7)	Ground Truth	But it's no use now, thought poor Alice, to pretend to be two people while there's hardly enough of me to make one respectable person.
	Predicted	But it's no use now, thought poor Alice, to pretend to be two people while there's hardly enough of me to make one respectable person.
(8)	Ground Truth	She was now only ten inches high, and her face brightened up at the thought that she was now the right size for going through the little door into that lovely garden.
	Predicted	She was now only ten inches high, and her face brightened up at the thought that she is now the right size for going through the little door into that lovely garden.
(9)	Ground Truth	for she had read several nice little histories about children who'd gotten burnt and eaten up by wild beasts and other unpleasant things.
	Predicted	for she had read several nice little histories about children who'd gotten burnt and eaten up by wild beasts and other unpleasant things.
(10)	Ground Truth	What a curious feeling, said Alice.
	Predicted	This time, she found a little bottle on it.
(11)	Ground Truth	Once or twice she peeped into the book her sister was reading.
	Predicted	Once or twice she peeped into the book her sister was reading.
(12)	Ground Truth	how she longed to get out of that dark hall and wander about among those beds of bright flowers and those cool fountains, but she could not even get her head through the doorway.
	Predicted	how she longed to get out of that dark hall and wander about among those beds of bright flowers and those cool fountains, but she could not even get her head through the doorway.
(12)	Ground Truth	Either the well was very deep, or she fell very slowly.
	Predicted	Either the well was very deep, or she fell very slowly.
(13)	Ground Truth	But alas for poor Alice, when she got to the door...
	Predicted	But alas for poor Alice, when she got to the door...
(14)	Ground Truth	For my end, you know, said Alice to herself, in my going out altogether like a candle.
	Predicted	For my end, you know, said Alice to herself, in my going out altogether like a candle.
(15)	Ground Truth	Do you think you could manage it?
	Predicted	Do you think you could manage it?

Table 11: Additional samples generated on *Brennan* dataset. **Bold** denotes a correct match.

(1)	Ground Truth	Roy stooped to pick up a big white rock that looked like a dirty lump of chalk and handed it to Chad
	Predicted	Roy stooped to pick up a big white rock that looked like a dirty lump of chalk and handed it to Chad
(2)	Ground Truth	Arthur and his wine
	Predicted	I may finish this story
(3)	Ground Truth	holding fidgeting conveyed glanced after sure rotting believing suppose water malignant replied
	Predicted	Holding fidgeting conveyed glanced after sure rotting believing suppose water malignant replied
(4)	Ground Truth	We spent the next hour stomping around the hill while he said things like it was right here
	Predicted	We spent the next hour stomping around the hill while he said things like it was right here
(5)	Ground Truth	there sounded slipped told mentioned for device issued all kentucky traffic whoever voice pushing
	Predicted	There sounded slipped told mentioned for device issued all kentucky traffic whoever voice pushing
(6)	Ground Truth	Collapsing at its base Allan wrapped his arms around the stoic tree and let forth a moan a cry of purest agony that escaped him as the first tears seeped from the corners of his eyes and slid down his cheeks falling to the ground and seeping though the fallen leaves and needles to join the water of the stream flowing through the ground beneath them
	Predicted	Collapsing at its base Allan wrapped his arms around the stoic tree and let forth a moan a cry of purest agony that escaped him as the first tears seeped from the corners of his eyes and slid down his cheeks falling to the ground and seeping though the fallen leaves and needles to join the water of the stream flowing through the grounds beneath them
(7)	Ground Truth	She seemed so self conscious and shallow on the outside but having that incredible gift
	Predicted	She seemed so self conscious and shallow on the outside but having that incredible gift
(8)	Ground Truth	It s hail across the and Tara spun to retake her seat at the helm
	Predicted	I shall consider it in the meantime however I must be off
(9)	Ground Truth	I put away the cell and used the motion to cover checking the knife in my sleeve and used one leg to check the other in my sock
	Predicted	But I always should come now immediately before the probe is reported late
(10)	Ground Truth	You could step on that marker and make the gestures the device and it would be like pushing a button in a very complex machine hu
	Predicted	It speaks to the deepest instinct within us all yet is entirely original
(11)	Ground Truth	destroyed another story last night
	Predicted	Destroyed another story last night
(12)	Ground Truth	Chad finished formula but this time he mind that Roy fell for it
	Predicted	Chad finished formula but this time he mind that Roy fell for it
(13)	Ground Truth	remote room voice truck would so what going silver taught screaming toads play being
	Predicted	Remote room voice truck would so what going silver taught screaming toads play being
(14)	Ground Truth	Tell them and they will create an audience
	Predicted	Tell them and they will create an audience
(15)	Ground Truth	Allan took a sandwich between his fingers
	Predicted	This is the ounces which I mentioned at the restaurant

Table 12: Additional samples generated on the *GWilliams* dataset. **Bold** denotes a correct match.

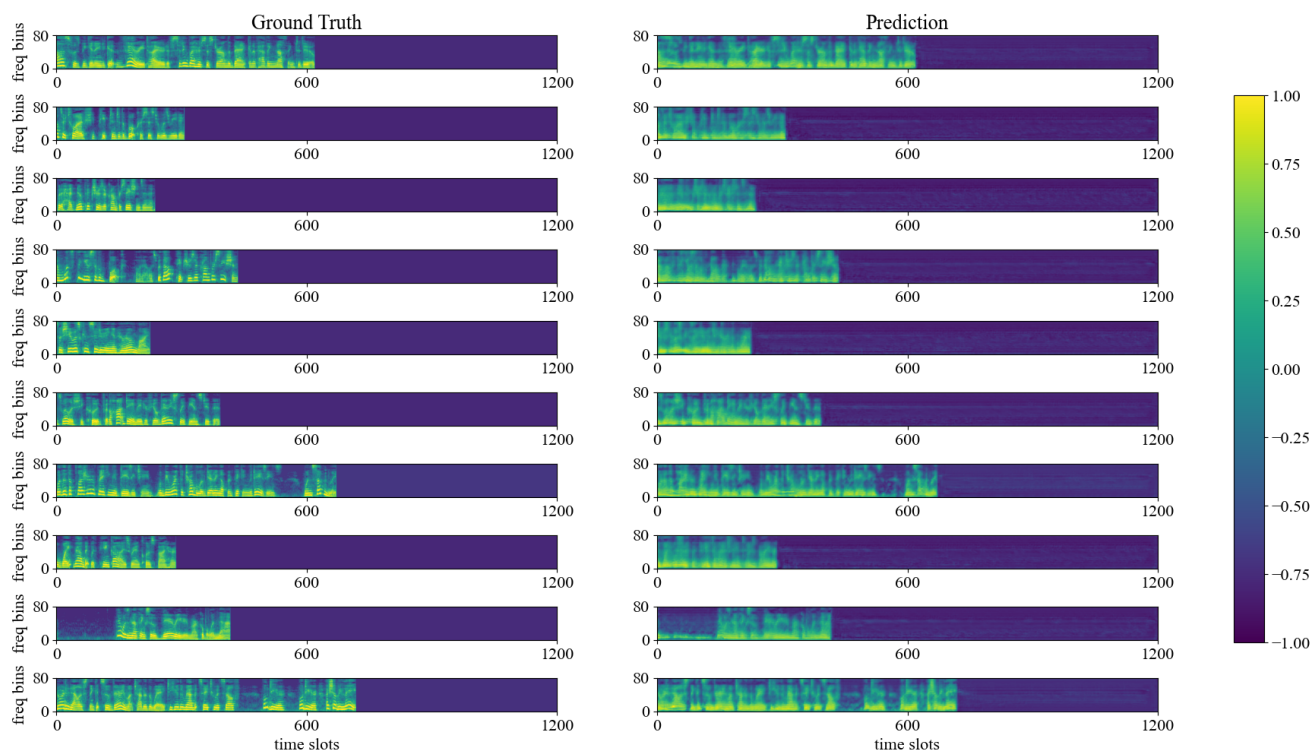


Figure 5: Predicted Mel spectrograms on *Brennan* dataset.

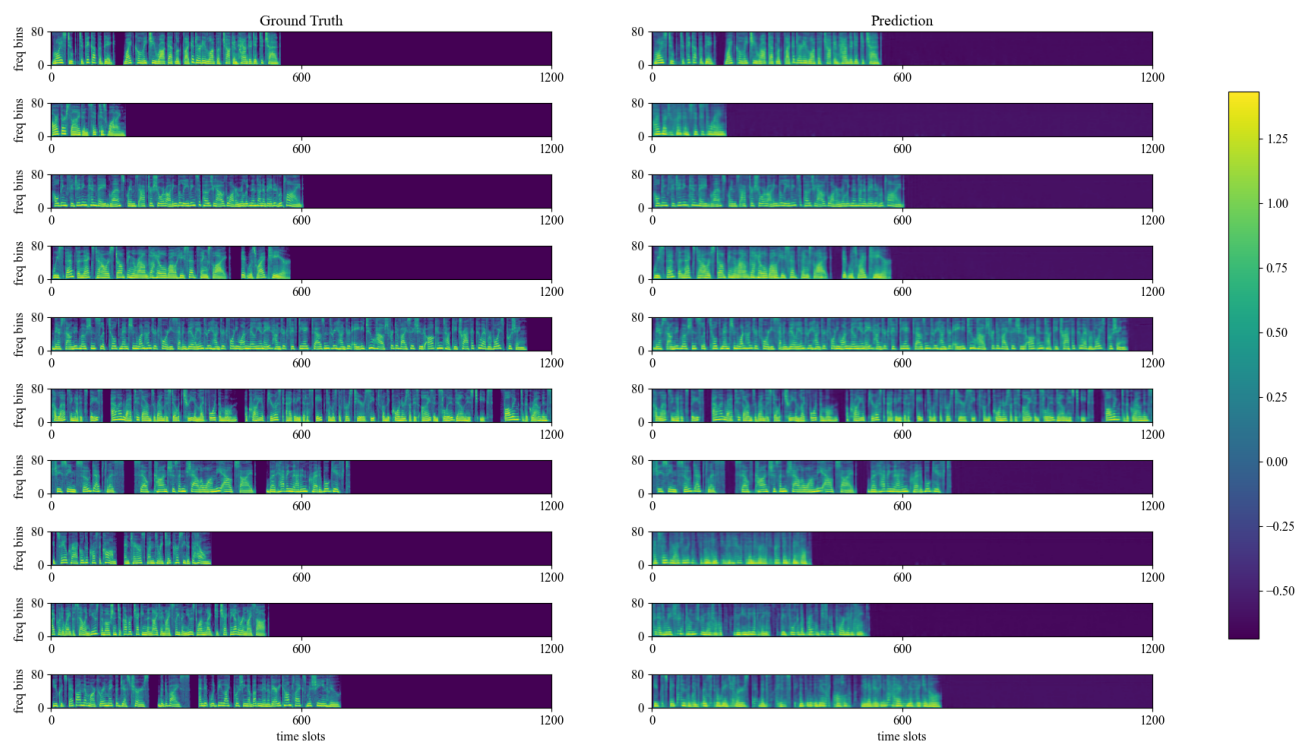


Figure 6: Predicted Mel spectrograms on the *GWilliams* dataset. For visualization purposes, only the first half of the Mel spectrograms are displayed.

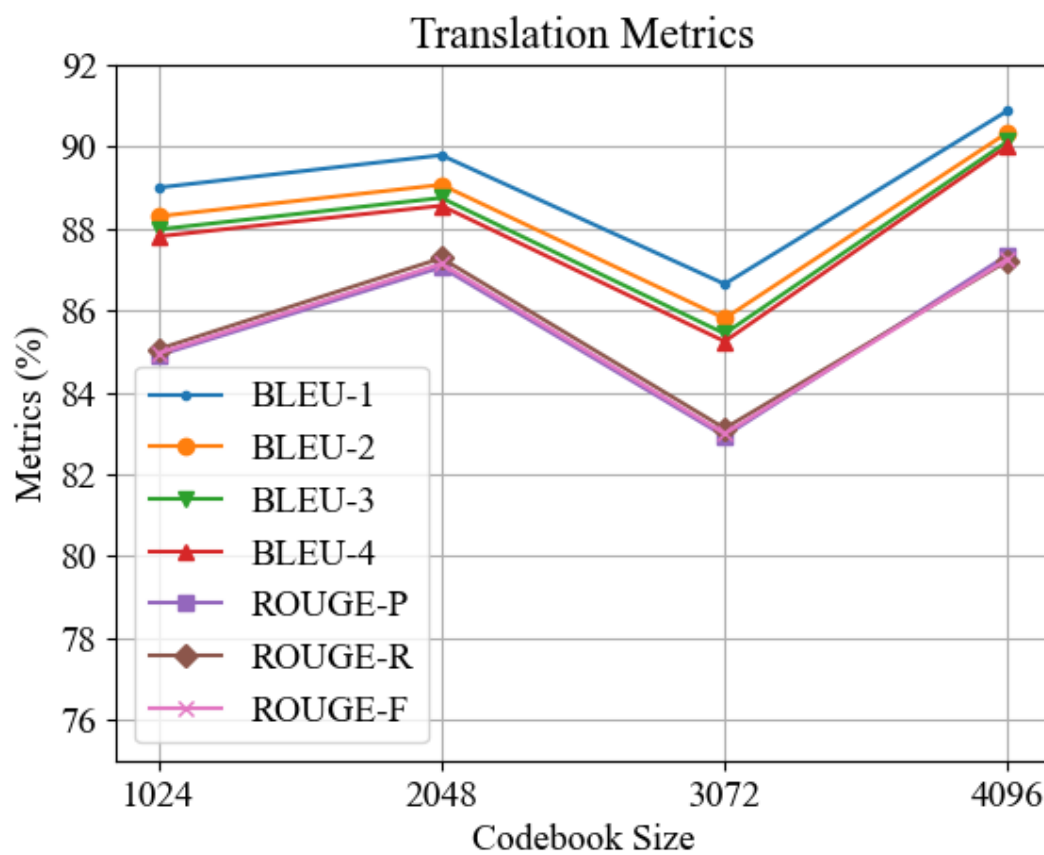


Figure 7: Translation performance using various codebook sizes on *Brennan* dataset.